Carbohydrate Polymers 151 (2016) 1073–1081

Contents lists available at ScienceDirect

Carbohydrate Polymers

journal homepage: www.elsevier.com/locate/carbpol

Influence of natural and synthetic crosslinking reagents on the structural and mechanical properties of chitosan-based hybrid hydrogels

I.M. Garnica-Palafox[a,b], F.M. Sánchez-Arévalo[a,*]

[a] Instituto de Investigaciones en Materiales, Universidad Nacional Autónoma de México, Apdo. Postal 70-360, Cd. Universitaria, Cd. de México 04530, Mexico
[b] Posgrado en Ciencia e Ingeniería de Materiales, Universidad Nacional Autónoma de México, Apdo, Postal 70-360, Cd. Universitaria, Cd. de México 04530, Mexico

ARTICLE INFO

Article history:
Received 26 February 2016
Received in revised form 7 June 2016
Accepted 8 June 2016
Available online 17 June 2016

Chemical compounds studied in this article:
Chitosan (PubChem CID: 71853)
Polyvinyl alcohol (PubChem CID: 11199)
Genipin (PubChem CID: 442424)
Glutaraldehyde (PubChem CID: 3485)

Keywords:
Chitosan
Poly(vinyl alcohol)
Hybrid hydrogels
Genipin
Glutaraldehyde

ABSTRACT

The objective of this work was to correlate the physical and chemical properties of chitosan/poly(vinyl alcohol)/genipin (CS/PVA/GEN) and chitosan/poly(vinyl alcohol)/glutaraldehyde (CS/PVA/GA) hydrogels with their structural and mechanical responses. In addition, their molecular structures were determined and confirmed using FTIR spectroscopy. The results indicated that the hybrid hydrogels crosslinked with genipin showed similar crystallinity, thermal properties, elongation ratio and structural parameters as those crosslinked with glutaraldehyde. However, it was found that the elastic moduli of the two hybrid hydrogels were slightly different: 2.82 ± 0.33 MPa and 2.08 ± 0.11 MPa for GA and GEN, respectively. Although the hybrid hydrogels crosslinked with GEN presented a lower elastic modulus, the main advantage is that GEN is five to ten thousand times less cytotoxic than GA. This means that the structural and mechanical properties of hybrid hydrogels crosslinked with GEN can easily be tuned and could have potential applications in the tissue engineering, regenerative medicine, food, agriculture and environmental industries.

1. Introduction

In recent years, natural and synthetic hydrogels have been developed to meet specific human requirements in different fields, such as the agricultural, environmental, food and even medical industries (Chawla, Srivastava, Pandey, & Chawla, 2014). The synthetic hydrogels that have frequently been used in the aforementioned fields are poly(ethylene glycol) (PEG), poly(ethylene oxide) (PEO) and poly(vinyl alcohol) (PVA) (Chawla et al., 2014). PVA has some particular advantages; among them, it has been reported to possess very low toxicity, hydrophilic behavior and a high elastic response. Nevertheless, PVA is soluble in water. This property could be disadvantageous for some applications; however, PVA has been widely used in applications such as articular cartilage and pancreas regeneration (Baker, Walsh, Schwartz, & Boyan, 2011; Paradossi, 2013, Chapter 2), drug-eluting contact lenses (Carreira et al., 2014), sensors for biological variables (Carmona, Martinez, Londo no, Montoya, & Torres, 2015; Tou, Koh, & Chan, 2014) and even for capturing organic dyes and metallic ions (Hui, Zhang, & Ye, 2015; Li, She, She, Dai, & Kong, 2014). Natural hydrogels such as collagen, gelatin, alginate, agarose and chitosan (CS) are very attractive and are commonly used for biological applications. These hydrogels take advantage of their excellent biocompatibility properties (Sionkowska, 2013, Chapter 11); however, natural hydrogels do not meet the load requirements for specific applications due to their poor mechanical properties. Furthermore, their mechanical properties have to be tuned.

The combination of synthetic and natural hydrogels has produced the so-called hybrid hydrogels; due to their easy preparation and the miscibility of PVA in CS, the CS/PVA blend is now one of the most used hybrid hydrogels (El-Hefian, Nasef, & Yahaya, 2010; Naveen Kumar et al., 2010). This blend benefits from the high elasticity of PVA and the good strength and biocompatibility of CS; therefore, the resulting blend, using the correct proportions of synthetic and natural hydrogels, could possess mechanical properties that are similar to those of human tissues. However,

* Corresponding author.
E-mail address: fsanchez@iim.unam.mx (F.M. Sánchez-Arévalo).

http://dx.doi.org/10.1016/j.carbpol.2016.06.036
0144-8617/

the long-term structural and mechanical stability of the blend is still an issue. To address this issue, chemical crosslinking reagents have been used (glutaraldehyde He & Xiong, 2012; Hu, Xin, Hu, Chan, & He, 2013, epichlorohydrin Garnica-Palafox et al., 2014 and genipin Bispo, Mansur, Barbosa-Stancioli, & Mansur, 2010; Khurma, Rohindra, & Nand, 2006). Recent efforts have demonstrated that the physicochemical properties of CS can be tuned, which has been achieved by combining CS with other polymers or using chemical crosslinkers. Interesting applications have been reported, such as genipin-crosslinked microgels from concanavalin A and glucosyloxyethyl acrylated chitosan for glucose-responsive insulin delivery (Yin et al., 2014) and a chitosan–hyaluronic acid polyelectrolyte complex scaffold crosslinked with genipin as a template for controlled bone morphogenetic protein-2 (BMP-2) delivery for bone tissue engineering (Nath, Abueva, Kim, & Lee, 2015). Mekhail, Jahan, and Tabrizian (2014) improved fibroblast attachment and proliferation using a hydrogel based on genipin-crosslinked chitosan/poly-L-lysine. Liu and Kim (2012) reported the antibacterial property of hydrogels based on CS/PEG doped with ZnO/Ag nanoparticles.

Although significant efforts have been devoted to understanding the behavior of hybrid hydrogels, only a few works have been devoted to exploring and correlating structural changes with the physical and chemical properties of CS/PVA hybrid hydrogels crosslinked with genipin (Bispo et al., 2010; Khurma et al., 2006). Moreover, the behavior of CS/PVA hydrogels crosslinked with genipin has not been fully explored. The aim of this work is to correlate the physical and chemical properties of chitosan/poly(vinyl alcohol)/genipin and chitosan/poly(vinyl alcohol)/glutaraldehyde hydrogels with their structural and mechanical responses allowing a better understanding of these hydrogels to tune their mechanical responses depending on the application that they have been selected for.

2. Materials and methods

The hydrogels were synthesized using deionized water and HPLC-grade acetic acid as solvents and using medium-molecular-weight chitosan powder (CS) with a 75–85% degree of deacetylation and poly(vinyl alcohol) (PVA) with a 99% degree of hydrolysis and a typical average molecular weight (Mw) of 89 000–98 000 g/mol. As chemical crosslinking reagents, analytical-grade genipin powder (GEN) and a 50% (wt.%) aqueous solution of glutaraldehyde (GA) were used. All chemicals were purchased from Sigma–Aldrich and were used directly as received.

2.1. Hydrogel preparation

The polymer hydrogels were prepared using the solvent casting method. A 10% (w/v) aqueous solution of poly(vinyl alcohol) was prepared by dissolving PVA in deionized water under magnetic stirring at 80 °C for 2 h. The chitosan solution was prepared by dissolving CS powder in a 1% (w/v) acetic acid solution under constant magnetic stirring at room temperature for 24 h to obtain a 2.5% (w/v) polymeric solution. Both polymeric solutions were carefully mixed at a volume ratio of CS/PVA of 3:1. The blend was stirred for 2 h at room temperature until the PVA and CS formed a clear solution. The resulting solution of CS/PVA was divided into two portions. One was crosslinked with GEN and the other one with GA in order to compare directly the effects of both crosslinkers. The genipin solution (0.5%, w/v) was prepared by dissolving GEN powder in deionized water at room temperature. Then, the crosslinking reagent (GEN) was slowly added to the CS/PVA base polymeric mixture, and it was stirred for 1 h at room temperature. The final concentration of GEN in the polymeric mixture was approximately 0.05% (w/v). Regarding CS/PVA/GA preparation the appropriate amount of GA (50% aqueous solution) was slowly added to CS/PVA base and the solution was stirred for 30 min at room temperature. The final concentration of GA in the polymeric mixture was the same used in the CS/PVA/GEN (i.e. 0.05%, w/v). Further in the sequence, a certain amount of the crosslinked polymeric solutions (13 g) was poured into plastic Petri dishes; they were subsequently dried for approximately 72 h at room temperature. The films of CS/PVA/GEN and CS/PVA/GA were carefully detached from the dishes and placed in a vacuum oven at 60 °C and −17 inHg for 48 h to remove the water and solvents inside the films. Finally, the thicknesses of films were measured using a digital micrometer (Mitutoyo), and then the films were stored in a desiccator until testing. We want to point out that pure CS, PVA and CS/PVA films were prepared with the same concentrations and conditions that were used to prepare the polymeric solutions of CS/PVA blend; these hydrogels were used as a control group for comparison purposes in all experiments.

2.2. Physical and chemical characterization

2.2.1. FT-IR spectroscopy

The obtained hydrogels were characterized using FT-IR spectroscopy to identify the polymer chemical groups, interactions between components (CS-PVA crosslinking reagent) and to elucidate the molecular structure of the crosslinked networks from films with GEN and GA. FT-IR spectroscopy was performed on dry samples with a thickness of 100 μm. This analysis was performed using attenuated total reflectance (ATR) with the following parameters: wavenumber range from 4000 to 400 cm^{-1}, 32 scans, and a resolution of 2 cm^{-1} (Nicolet 6700, Thermo Scientific). The measured FT-IR spectra were normalized, and major vibrational bands were identified and associated with the main chemical groups.

2.2.2. Swelling test

The swelling properties of pure polymer hydrogels, CS/PVA blend hydrogels and crosslinked hydrogels (CS/PVA/GEN and CS/PVA/GA) were studied by immersing the samples in phosphate buffered saline (PBS) (pH 7.4) at 37 °C. Five square samples, with a side length of 10 mm, were cut from each group of dried hydrogels. At fixed time intervals, the specimens were removed from the PBS and they were carefully wiped using filter paper in order to remove the free water on the surface of the hydrogels; subsequently, the samples were weighed and then returned to the same container. In this way, the swelling test only considered the interstitial water trapped in the polymeric network and the bound water directly attached to the polymer chains through hydration of functional groups according to Omidian and Park (2010, Chapter 1). The swelling ratio (%*S*) was calculated using Eq. (1), according to Garnica-Palafox et al. (2014):

$$S\ (\%) = \frac{W_s - W_d}{W_d} * 100 \quad (1)$$

where W_s is the weight of swollen samples at different swelling time intervals and W_d corresponds to the weight of the completely dried sample. The time intervals, in minutes, were as follows: 2.5, 5, 7.5, 10, 12.5, 15, 20, 25, 30, 45, 60, 120, 180, 240, 320, 1440 and 2880.

2.2.3. Contact angle measurements

The contact angles of water on the hydrogel films were measured in the dry state, at room temperature, using the sessile drop method (Yuan & Lee, 2013, Chapter 1) A small drop (0.5 μl) of deionized water was carefully deposited onto the surface of a square hydrogel sample with a side length of 5 mm. Then, a series of pictures of the drop on the film were acquired to measure the angle

formed between the drop edge and the hydrogel surface. These angles were measured from both sides of the drop using a set of consecutive images, which were registered by a CCD camera coupled to an optical microscope; using digital image analysis, the images were digitally filtered for edge detection and angle measurements were carried out using a Matlab scrip. The average contact angle for each hydrogel was reported.

2.2.4. X-ray diffraction measurements

The crystallinities of the pure CS and PVA hydrogels and of the CS/PVA blend and its crosslinked blends (CS/PVA/GEN and CS/PVA/GA) were analyzed using X-ray diffraction with an X-ray diffractometer (Bruker D8 Advance) operating at 45 kV with Ni-filtered $CuK\alpha_1$ radiation ($\lambda = 1.5406$ Å). Diffraction patterns were recorded over the 2θ range of 5–70° with a scan rate of 0.4°/min. The crystallinity (%) was calculated using a cut and weight method via Eq. (2), as reported by Zheng, Du, Yu, and Xiao (2000):

$$C\ \ (\%) = \frac{A_c}{A_a + A_c} * 100 \tag{2}$$

where A_c is the area under the curve (X-ray diffraction pattern) that corresponds to crystalline zones and A_c is the area under the curve that corresponds to amorphous regions within the hybrid hydrogel.

2.2.5. Thermal characterization

The melt and glass transition behaviors of the CS/PVA hydrogels and their blends crosslinked with GEN and GA were studied using a differential scanning calorimeter (DSC, Q100 TA Instruments) under a nitrogen atmosphere. First, 10 mg of sample was sealed in an aluminum pan and heated from 20 to 150 °C at a heating rate of 10 °C/min; the sample was held at 150 °C for 2 min and then cooled to room temperature to eliminate the moisture inside the polymeric network and to release the internal stress of the sample. Second, the sample was heated again from 50 to 250 °C at a heating rate of 10 °C/min. The second heating was recorded and used for the analysis.

2.2.6. Mechanical characterization and structural parameters

Synthesized polymer films of CS, PVA, CS/PVA, CS/PVA/GEN and CS/PVA/GA were hydrated until equilibrium. Then, the samples were cut into a dog-bone shape using a special jig according to the ASTM D1708 standard (ASTM-International, 2013). The thickness of each sample was measured along three different positions using a Mitutoyo digital gauge to obtain an average measurement for the thicknesses of the samples. Next, the samples were held between the grips of a custom-designed tensile device and stretched at a constant rate of 0.16 mm/seg. Five samples of each hybrid hydrogel were tested under uniaxial tension at 24 °C using a gauge length of 21 mm. With the recorded displacement and force data, a curve of macroscopic stress (σ) vs. elongation ratio (λ) was obtained for each case. From these curves, mechanical properties such as shear modulus (μ), maximum stress and maximum elongation ratio of the hydrogels were determined using a first-order model for large deformation for incompressible rubber-like solids under uniaxial tension (shown in Eq. (3)), as previously reported by Ogden (1973).

$$\sigma(\lambda) = \frac{2\mu}{\alpha}(\lambda^{\alpha-1} - \lambda^{-(1/2)\alpha-1}) \tag{3}$$

where σ is the stress, λ is the elongation or elongation ratio ($\lambda = \epsilon + 1$), μ is the shear modulus, and α is a parameter related to the strain invariants for incompressible materials according to the strain energy function proposed by Ogden. Using data from the uniaxial tensile experiments and considering the Ogden model, the parameters μ and α can easily be estimated by non-linear fitting. Now taking into account that hydrogels can be considered as incompressible materials, the elastic modulus (E) can be calculated as $E = 3\mu$ (Treloar, 2005). Finally, the maximum elongation ratio (λ_{max}), which refers to the strain of the sample just before it breaks, was calculated using Eq. (4).

$$\lambda_{max} = \frac{l_{max} - l_0}{l_0} + 1 \tag{4}$$

where l_{max} is the length of the sample at the breaking point and l_0 corresponds to the sample length before being deformed.

2.3. Structural properties

The mechanical behavior of hydrogels can also be modified by three structural parameters of their polymeric network, namely, the average molecular weight between crosslink points (M_{crl}); the correlation length (D_N), also known as the network mesh or pore size; and the equilibrium polymer volume fraction in the swollen state (V_s) Peppas and Mikos (1987). The shear modulus, which was experimentally obtained in the previous section, can be used to calculate these structural features of the polymeric network. The average molecular weight (M_{crl}) was calculated using statistical theory, considering Eq. (5), according to Mathews, Birney, Cahill, and McGuinness (2008):

$$M_{crl} = \frac{cRT}{\mu} \tag{5}$$

where c is the concentration (g/m^3) of CS and PVA in the crosslinking solution, T is the temperature in Kelvin at which the shear modulus was determined, and R is the gas constant (8.3145 J/mol K). Additionally, D'Errico et al. (2008) showed that the network mesh size (D_N) can be calculated using Eq. (6), which is the *equivalent network model* reported by Flory (1953, Chapters 11 and 12). The network mesh size is indicative of the average distance between consecutive crosslink points. According to Eq. (5), (D_N) can easily be determined if the concentration (c) and the number-average molecular weight (M_{crl}) are known

$$D_N = \sqrt[3]{\frac{6M_{crl}}{\pi A * c}} \tag{6}$$

where A is Avogadro's number (6.023×10^{23} mol^{-1}).

3. Results and discussion

3.1. Structure of the hydrogels

Fig. 1(a) and (b) show the structural characterization of pure CS and PVA and their different blends. In particular, changes in the molecular structure in the CS/PVA base blend films and in the CS/PVA/GEN and CS/PVA/GA crosslinked hydrogels can be observed; these changes were registered by FT-IR analysis. According to these results, it was possible to propose the molecular structures of the crosslinked hydrogels, which are presented in Fig. 1(c) and (d). The FT-IR spectra of pure films of CS (top curve) and PVA (bottom curve) are shown in Fig. 1(a); both of these films were used as control/reference samples. The CS sample exhibited characteristic peaks ranging between 3500 and 3300 cm^{-1}, which correspond to the N–H/O–H stretching vibration mode. Additionally, peaks corresponding to amides I, II, and III and of N–H out-of-plane vibration were identified at 1650, 1550, 1322 and 640 cm^{-1}, respectively. This result was previously reported by Costa-Júnior, Barbosa-Stancioli, Mansur, Vasconcelos, and Mansur (2009). Finally, peaks corresponding to the C–O stretching mode were located at 1030 and 1070 cm^{-1}, which is in good agreement with the results reported by Yao, Liao, Chung, Sung, and Chang (2012). The FT-IR spectrum of pure PVA also presented characteristic bands for hydroxyl groups at 3400 cm^{-1}, for the stretching

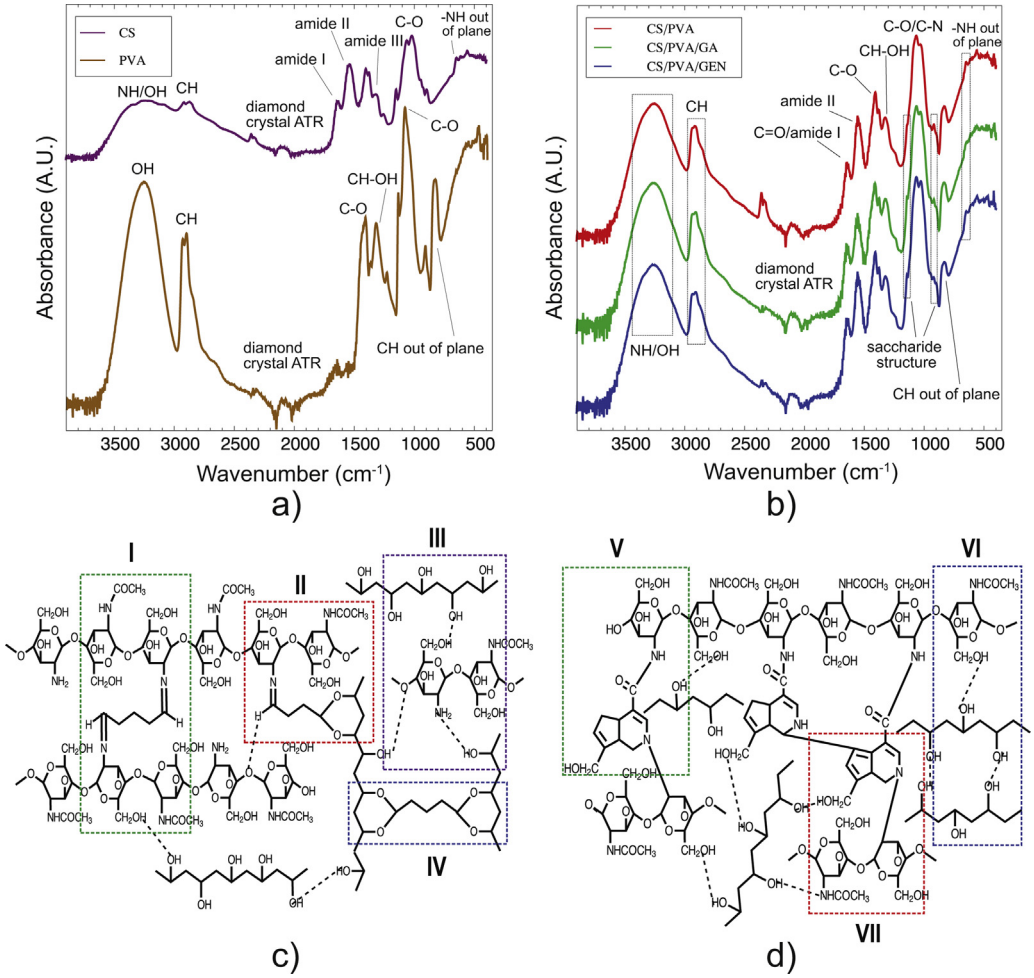

Fig. 1. FT-IR spectra and proposed molecular structures of crosslinked hydrogels are presented for both crosslinker reagents (GEN and GA); the crosslinking reactions were carried out at pH 4 and the blends were stirred for 1 h at room temperature. (a) FT-IR spectra of pristine polymers: CS and PVA. (b) FT-IR spectra of polymer blends: CS/PVA, CS/PVA/GA and CS/PVA/GEN. (c) Proposed molecular structure of CS/PVA hydrogels crosslinked by GA. (d) Probable molecular structure of CS/PVA hydrogels crosslinked by GEN.

vibrational mode for C–H bonds at 2900 cm^{-1}, and for the stretching vibrational modes for C–O bonds at 1400 and 1090 cm^{-1}. These bands were previously reported by Costa-Júnior et al. (2009) and El-Hefian et al. (2010).

After the typical FT-IR vibrational bands of pure CS and pure PVA were separately identified, FT-IR analyses of CS/PVA crosslinked blends were performed. Fig. 1(b) shows the main vibrational bands for these blends. The FT-IR spectra of CS/PVA, CS/PVA/GA and CS/PVA/GEN (top, middle and bottom curves, respectively) are shown in Fig. 1(b). The main change of the CS/PVA blend, with respect to the separate pure polymers, was detected as an increase in absorbance. This increase was due to the formation of inter- and intramolecular hydrogen bonds as a consequence of the interaction between the OH and NH groups of PVA and CS, respectively; this result is consistent with a previous one reported by Costa-Júnior et al. (2009). Regarding the CS/PVA blend and the glutaraldehyde-crosslinked hydrogel, a decrease in the absorbance at 3500–3000 cm^{-1} was observed because of the effect of the chemical crosslinking reagent. This produced Schiff bases and acetal groups in the new network; in this way, the band located at 1030 cm^{-1}, which is associated with C–O bonds, registered as an absorbance increase due to the formation of acetals. Additionally, a small shoulder was detected at 1630 cm^{-1}, which corresponds to the imines of Schiff bases. Another contribution of GA as crosslinking reagent was detected at 640 cm^{-1}; here, the band corresponding to primary amines was inhibited. Meanwhile, the CS/PVA blend crosslinked with genipin (GEN) showed the main changes at 1090 and 1070 cm^{-1}, which correspond to the formation of C–N bonds. Subsequently, a decrease in absorbance at 1570 and 640 cm^{-1} was observed. This decrease was associated with primary amines and with the formation of a new band at 1650 cm^{-1}, which corresponds to the formation of amide-type bonds. Good agreement was found with recent research reporting the FT-IR spectra for CS/PVA/GA by Hu et al. (2013), Mansur, Costa-Junior, Mansur, and Barbosa-Stancioli (2009) and CS/PVA/GEN by Bispo et al. (2010), Muzzarelli (2009).

Although previous research has reported FT-IR analyses for CS/PVA, CS/PVA/GA and CS/PVA/GEN crosslinked blends, their molecular structures have not been completely understood. Furthermore, we proposed the possible structures of the crosslinked hydrogels. Fig. 1(c) depicts the possible molecular structure of the CS/PVA/GA blend. The region marked with number I corresponds to the bonds obtained due to the interaction between GA and $-NH_2$ of two chains of CS producing two Schiff bases; this matched with a small shoulder located at 1630 cm^{-1} that corresponds to the formation of imines (middle curve shown in Fig. 1(b)). Region II shows the CS and PVA chains bound by an acetal group and a Schiff base, as previously discussed in Fig. 1(b) at 1030 and 1630 cm^{-1}, respectively. Moreover, region III indicates inter- and intramolecular hydrogen bonds between CS and/or PVA chains. The

last region for the CS/PVA/GA blend, marked with number IV, illustrates the bonds between two chains of PVA through acetal groups. Now, when genipin was used as a crosslinking reagent, the molecular structure experienced considerable changes with respect to the CS/PVA/GA molecular structure. These changes are observed as amide-type bonds (region V shown in Fig. 1(d)) that match with a band at 1650 cm^{-1} in the bottom curve of Fig. 1(b). Additionally, region VI depicts the inter- and intramolecular hydrogen bonds between CS and PVA chains. Finally, bonds between CS chains with heterocyclic compounds due to the dihydropyran ring opening of genipin are represented in region VII of Fig. 1(d) and are observed at 1090–1070 cm^{-1} in the bottom curve of Fig. 1(b).

3.2. Physical properties of the hydrogels: swelling, contact angle, crystallinity and thermal behavior

Because of the changes observed in the molecular structures of the obtained hybrid hydrogels (CS/PVA, CS/PVA/GA and CS/PVA/GEN), their physical properties, such as swelling behavior, contact angle, crystallinity and thermal behavior, were studied. Fig. 2(a) shows the swelling behaviors of pure CS and PVA and of their blends that were crosslinked with GA and GEN. This chart presents the percentage of swelling as a function of time, showing that pure CS hydrogels were able to swell in PBS and they exhibited a maximum swelling capacity of 745% at 2.5 min; after this maximum swelling, the water uptake percentage of pure CS hydrogels decreased until equilibrium was reached (490% at 60 min). This swelling capacity at equilibrium was in good agreement with the reported by Giovino, Ayensu, Tetteh, and Boateng (2013). The swelling-deswelling behavior (overshooting effect) of CS hydrogels embedded into PBS can be well explained by the polymer-water interactive forces and the osmotic pressure gradient. On one hand, the hydrophilic groups (amino and hydroxyl) present in the backbone of chitosan are able to interact with water molecules present in the PBS solution through hydrogen bonds; this produces the swelling of the polymeric network. On the other hand, due to the CS hydrogels structure contains ionic groups (NH_2^+), an osmotic pressure gradient is generated because of the difference in ion concentration within the gels and the outside PBS solution (Na^+, Cl^- and K^+). As hydrogels swells the osmotic pressure decreases and eventually the swelling equilibrium is reached (Berger et al., 2004; Garnica-Palafox et al., 2014). So, the greater the difference in the ion concentration is, the larger the osmotic pressure becomes, causing a larger equilibrium water uptake of hydrogel sample (Gupta & Shivakumar, 2012). The swelling capacity at equilibrium of pure PVA hydrogels films was 175%. It is known that PVA has multitude of hydroxyl groups; between them, can occur inter and intra molecular hydrogen bonding producing a sort of crosslinking action; nevertheless, some of them remain free to interact with water molecules into the PBS solution and allow for swelling PVA polymeric network (Omidian & Park, 2010, Chapter 1). The CS/PVA blend exhibited the maximum swelling (1040%) capacity at 2.5 min; subsequently, equilibrium was reached after 180 min, registering a swelling of 500% (even after 3 days). The swelling capacities at equilibrium of the CS/PVA/GA and CS/PVA/GEN hydrogels were 190 and 270%, respectively. Hence, the GA and GE crosslinking reagents decreased the swelling capacities of the hydrogels; nonetheless, the crosslinking reaction was necessary because CS, PVA, and CS/PVA hydrogels dissolve at specific conditions in some liquids, such as water or diluted acid solutions, after few days. Thus, these results demonstrated that the chemical crosslinking reagents had a significant effect on the network producing a more stable material in wet state.

The FT-IR results demonstrated that OH and NH hydrophilic groups were consumed during the crosslinking reaction, producing new chemical bonds and therefore more rigid films. It was observed that the mobility and deformation of their polymeric chains were significantly reduced; hence, the network lost water absorption capability. Comparing the swelling behavior between CS/PVA with the CS/PVA/GA and CS/PVA/GEN blends, it was found that the overshooting effect, which was reported for CS and CS/PVA blend by Garnica-Palafox et al. (2014), was inhibited because of the chemical crosslinking reagents.

Table 1
Percentage of crystallinity obtained by X-ray diffraction measurements.

Sample	(%) Crystallinity
CS	17 ± 0.7
PVA	28 ± 5
CS/PVA	21.5 ± 2
CS/PVA/GA	17 ± 0.4
CS/PVA/GEN	16.8 ± 0.6

Fig. 2(b) shows the hydrophilic behaviors of pure CS, PVA, CS/PVA and their crosslinked blends. This figure shows that pure CS and PVA presented hydrophilic behavior; however, CS presented a larger contact angle (72 ± 2°) than PVA (40 ± 1°). When CS and PVA were mixed, the contact angle of the CS/PVA blend was 65 ± 1°. For the CS/PVA/GA and CS/PVA/GEN blends, it was observed that the GA and GEN crosslinking reagents had no considerable effect on the hydrophilicity of these hydrogels (64 ± 1° and 63 ± 1°, respectively).

Fig. 2(c) shows the X-ray diffraction patterns, in which the typical crystalline peaks of pure CS and PVA and their blends are observed. The diffraction pattern of CS presented four peaks at 2θ values of 10°, 20°, 21.7° and 40.5°, which correspond to the (020), (200), (201) and (143) diffraction planes, respectively; this result is in accordance with JCPDS 39-1894 and Mogilevskaya, Akopova, Zelenetskii, and Ozerin (2006). Ogawa, Yui, and Miya (1992) reported that the first two peaks correspond to a hydrated form of CS. The diffraction pattern of PVA presented peaks at 2θ values of 12°, 20°, 23.4° and 41°; these peaks corresponded to diffraction planes of (100), (101), (200) and (111), respectively, according to Hyon, Chu, and Kitamaru (1975) and Li et al. (2014). From the X-ray diffraction pattern located in the middle of Fig. 2(c), it can be observed that the peak associated with CS (at 10°) disappeared; in addition, the full width at half maximum (FWHM) of the peaks close to 20° increased. This result demonstrated that CS and PVA are miscible enough to produce strong interactions between CS and PVA molecules. Moreover, the crosslinked samples (CS/PVA/GA and CS/PVA/GEN) presented a small left shift on their first peak located at $2\theta = 12°$ with respect to the CS/PVA blend; this again indicates the miscibility between components and also indicates the action of the crosslinking reagent over the CS/PVA blend. The most intense peak also experienced a small left shift (at $2\theta = 19°$), and its FWHM also increased; this result is due to the increase of amorphous regions. This result was expected because the crosslinking reagent hinders the arrangement of polymer chains (Costa-Júnior et al., 2009). Hence, the use of a crosslinking reagent decreased the crystallinity of the hydrogels; in other words, these reagents inhibited the folding of polymer chains that is responsible for producing crystalline regions in the polymeric network. The crystallinity values are summarized in Table 1.

The thermal analysis results are presented in Fig. 2(d), and these curves present the heat flow as a function of temperature. Here, the critical temperatures (T_g and T_m) of the hydrogels were identified. The first zone labeled with letter *i* corresponds to T_g (glass transition temperature). Zone *ii*, which is defined by a small endothermic peak, indicates the melting temperature T_x of new crystalline regions that were obtained during the first cycle of heating (used to evaporate water). Zone *iii* shows the endothermic peaks associated with the melting point of the hydrogels. Note that the

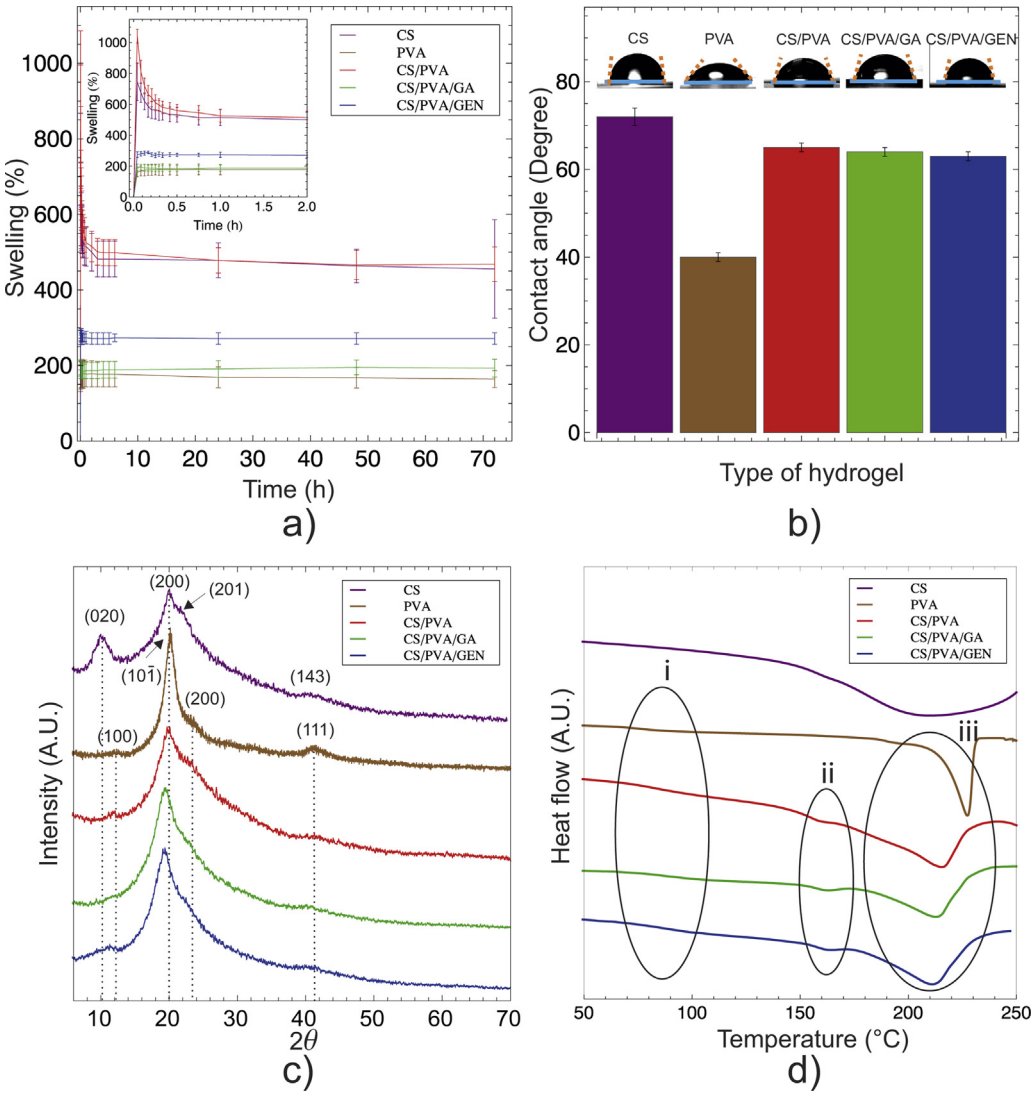

Fig. 2. Structural and physical characterization of hydrogels. (a) Swelling behaviors of CS, PVA, CS/PVA, CS/PVA/GA and CS/PVA/GEN hydrogels during 70 h; the swelling properties of hydrogels were studied by immersing the samples in PBS (pH 7.4) at 37 °C. (b) Contact angles of pristine polymers, blend polymer and blend polymer crosslinked by GA or GEN; the contact angles were measured at room temperature using a small drop (0.5 μl) of deionized water onto the surface of hydrogels in dry state. (c) X-ray diffraction pattern of hydrogels; the essay was carried out at room temperature. (d) DSC of CS, PVA, CS/PVA, CS/PVA/GA and CS/PVA/GEN hydrogels; these thermograms correspond to the second heating cycle that was carried out at 10 °C/min from 50 to 250 °C.

Table 2
Critical temperatures of CS, PVA and their crosslinked blends.

Sample	T_g °C	T_x °C	T_m °C
CS	–	–	–
PVA	75 ± 0.5	–	227 ± 0.5
CS/PVA	84 ± 0.5	159 ± 0.1	216 ± 0.5
CS/PVA/GA	87 ± 4	162 ± 1.7	214 ± 1.4
CS/PVA/GEN	89 ± 5	163 ± 1	213 ± 2.3

T_g value for pure CS was not clearly observed in our measurements; however, Chuang, Young, Yao, and Chiu (1999) reported that this temperature is approximately 21 °C. Likewise, the melting temperature of pure CS was not detected; it was found in the literature (Chuang et al., 1999; El-Hefian et al., 2010) that polysaccharides do not present a well-defined melting temperature and rather present a gradual degradation temperature; in particular, our pure CS exhibited gradual degradation after 150 °C. The pure PVA clearly showed the T_g and T_m, which were 75 and 227 °C, respectively.

From Table 2 and Fig. 2(d), changes in T_g and T_m were observed. The glass transition temperature increased by 3.3 and 5% for the crosslinked hydrogels (GA and GEN, respectively) compared to the CS/PVA sample. This increase is related to the effect of the crosslinking reagent and therefore to the mobility of polymeric chains inside the network. Hence, adding GA or GEN will produce more rigid networks, and higher temperatures will be required to initiate movement between chains. Regarding T_m, it was found that the crosslinked blends showed a decrease in T_m ranging between 1.7 and 3.3 °C compared with CS/PVA; this result indicates good miscibility due to the presence of molecular interactions between CS/PVA and the crosslinking reagents. From these endothermic peaks, the associated enthalpy was calculated; the following average values were found: 39.3 ± 2.6, 31.4 ± 3.2 and 32.9 ± 7.3 J/g for CS/PVA, CS/PVA/GA and CS/PVA/GEN, respectively. Hence, the addition of crosslinking reagents decreased the enthalpy associated with T_m; the same trend for the (%) of crystallinity was also observed during the X-ray diffraction analysis. These results showed that the crosslinked hydrogels have almost the same crystalline/amorphous ratio. Nevertheless, changes in their mechanical behavior could be expected.

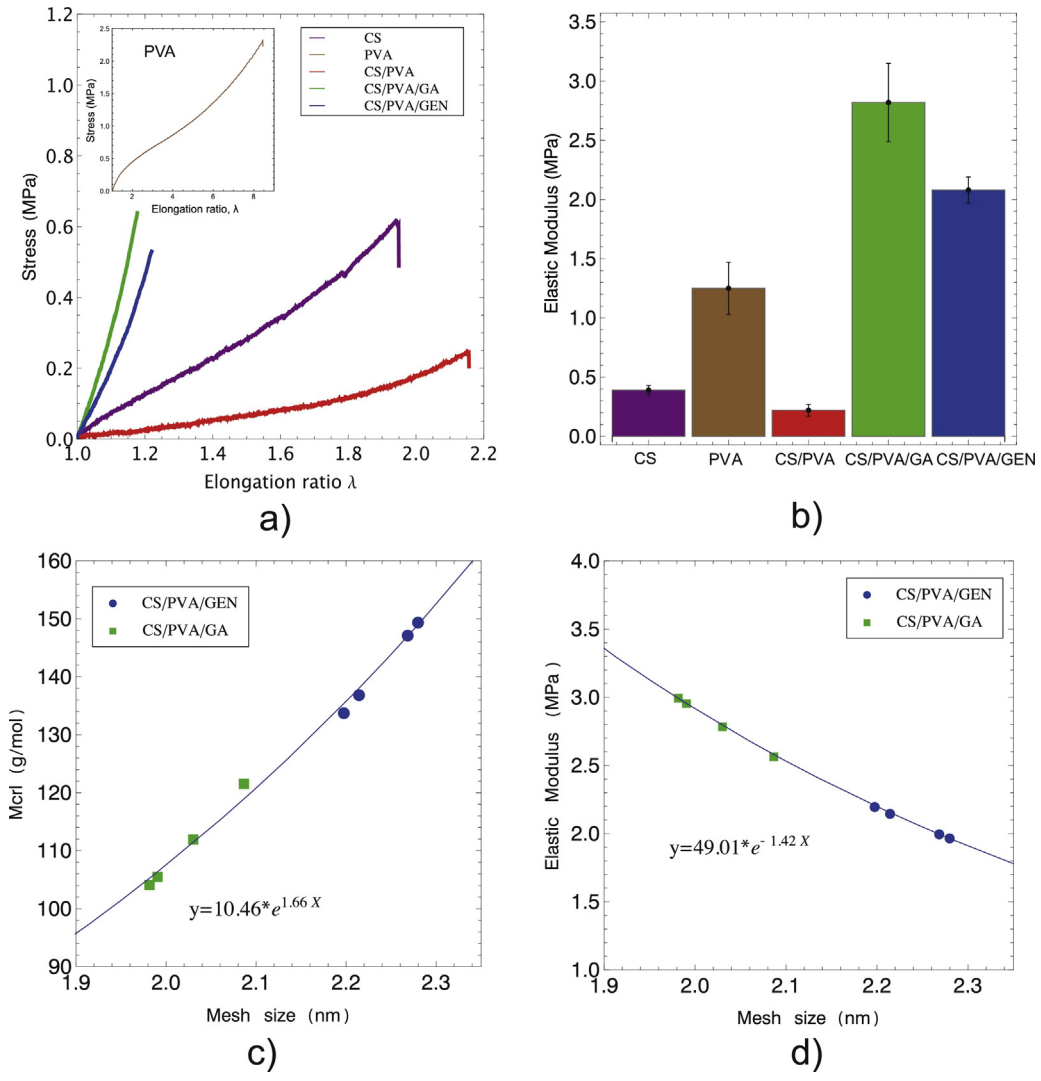

Fig. 3. Mechanical behaviors of CS, PVA, CS/PVA, CS/PVA/GA and CS/PVA/GEN hydrogels; the mechanical tests were carried out at room temperature (24 °C) using a strain rate of 0.16 mm s^{-1}. (a) Stress as a function of elongation ratio (λ); the inset shows the behavior of PVA hydrogels. (b) Comparative chart of the elastic moduli of the hydrogels. (c) M_{crl} as a function of mesh size. (d) Elastic modulus as a function of mesh size.

3.3. *Mechanical properties under uniaxial tensile test*

Fig. 3(a) shows the mechanical behaviors under uniaxial tension of pure CS and PVA hydrogels, the base-blend (CS/PVA) and their crosslinked blends (CS/PVA/GA and CS/PVA/GEN). In this figure, the stress as a function of elongation ratio (λ) curves are presented for each hydrogel. The obtained curves showed that the mechanical behaviors of all tested hydrogels, in the hydrated state, were non-linear. This result means that these hydrogels will present a rubber-like behavior, and it will primarily depend on the architecture of the polymeric network. The pure PVA hydrogels showed an average maximum elongation ratio of 8.5 ± 0.01 (shown in the inset of Fig. 3(a)), whereas the average maximum elongation ratio of the CS hydrogels was only 1.8 ± 0.23. Note that when both polymers were blended, the CS/PVA hydrogels showed a maximum elongation ratio equal to 2 ± 0.18; representing an increment of 0.2 respect to maximum elongation ratio of pure CS hydrogels. This result indicates that adding PVA to CS will improve the elasticity of the blend. In contrast, when the base blend was crosslinked with GA or GEN, a noticeable decrease in their maximum elongation ratio was observed (also shown in Fig. 3(a)). The average of maximum elongation ratio for the CS/PVA/GA and CS/PVA/GEN hydrogels were 1.14 ± 0.02 and 1.16 ± 0.04, respectively. This was due to the effect of the crosslinking reagents that modified the network architecture, as previously suggested in Fig. 1(c) and (d). The chemical reagents produced crosslinking points between polymeric chains, which inhibited the movement and unfolding of chains within the network. Due to the nonlinear mechanical behavior of hydrogels, the shear moduli (μ) of the hydrogels were calculated using Ogden's model (Ogden, 1973); subsequently, the elastic modulus was obtained by $E = 3\mu$ (Treloar, 2005). Fig. 3(b)) shows a comparative analysis between the elastic moduli (E) of pure CS and PVA, as well as, their crosslinked blends. The pure CS hydrogels in the hydrated state had an elastic modulus of 0.39 ± 0.04 MPa, whereas PVA presented an elastic modulus of 1.25 ± 0.22 MPa; this is in good agreement with a previous result reported by Oliveira et al. (2014). The elastic modulus of the base blend was 0.22 ± 0.05 MPa, whereas the blends crosslinked with GA and GEN presented elastic modulus values of 2.82 ± 0.33 MPa and 2.08 ± 0.11 MPa, respectively. These results demonstrate that GA and GEN enhanced the mechanical properties (elastic modulus and UTS) of the base blend; nevertheless, the elongation ratio was significantly reduced. From Fig. 3(b)), it is evident that GA was more effective in increasing the elastic modulus than GEN, but GA is more cytotoxic than GEN.

Furthermore, GEN will be the most suitable crosslinking reagent if a good balance between cytotoxicity and mechanical properties is considered.

3.4. Structural parameters of polymer network

Knowing the shear modulus and the chemical composition of the hybrid hydrogels, some of their physical properties, such as the effective molecular weight between crosslinking points and network mesh size, can be estimated using an exponential fitting.

Fig. 3(c) shows the relationship between two structural parameters of the network: the effective molecular weight between crosslinking points (M_{crl}) and the network mesh size (D_N). According to Flory (1953, Chapters 11 and 12), D_N is indicative of the average distance between consecutive crosslinking points, whereas M_{crl} is the average molecular weight of chains that form the polymeric network. In this way, we obtained average values of 111 ± 8 g/mol and 141 ± 8 g/mol for M_{crl} and mesh sizes of 2 ± 0.05 nm and 2.2 ± 0.04 nm for CS/PVA/GA and CS/PVA/GEN, respectively.

From the effective molecular weight between crosslinking points as a function of the mesh size curve, it is observed that M_{crl} increases exponentially as the mesh size (D_N) increases; this means that changing the crosslinking reagent (type/quantity) will modify the swelling ratio. Consequently, the length of polymeric chains will also be modified; a larger mesh size will trap more molecules of water. In other words, a high degree of swelling at equilibrium is generally associated with a large pore and high M_{crl}; this is in agreement with the swelling percentage shown in Fig. 2(a). The mechanical behavior of hydrogels could also be described in terms of the polymeric network structure. Fig. 3(d) shows that the elastic modulus decreases exponentially as D_N increases. This result means that a polymer with a greater mesh size, such as CS/PVA/GEN hydrogels, will present a lower elastic modulus. This is because a small mesh size will form a more rigid polymeric network, which will offer a higher strength; it is due to crosslinking points being closer and restricting the movement of polymer chains. According to these results, we can state that the mechanical properties of the hydrogels, such as the elastic modulus, are governed by their structure at the microscopic level or equivalently by the molecular weight between crosslinking points (M_{crl}) and D_N.

4. Conclusions

Crosslinked hybrid hydrogel films (CS/PVA/GEN and CS/PVA/GA) were successfully obtained using the solvent casting method. FT-IR analysis showed that intermolecular interactions exist between PVA and/or CS molecules due to crosslinking reagents, which created stronger 3D polymeric networks than in the CS/PVA-based polymeric blend. The use of the crosslinking reagents GA and GEN on the CS/PVA blend reduced its swelling capacity by 62 and 46%, respectively. In addition, it was found that the overshooting effect on the swelling behavior of the CS/PVA blend was inhibited by these crosslinking reagents. It was demonstrated that GA and GEN had no significant influence on the contact angle value. Incorporating GA and GEN chemical crosslinking reagents reduced the percentage of crystallinity of the CS/PVA blend by 21% and 22%, respectively, but increased the glass transition temperature by approximately 3.3% and 5%, respectively. Regarding the mechanical response of CS/PVA and crosslinked hydrogels (CS/PVA/GA and CS/PVA/GEN), particularly the Young's modulus, it was increased by up to ten-fold by using the aforementioned chemical crosslinking reagents. In brief, CS/PVA/GEN and CS/PVA/GA hydrogels provided superior physical, chemical, and mechanical properties in wet state than CS/PVA.

The CS/PVA/GEN and CS/PVA/GA hydrogels exhibited similar physical, thermal and polymeric network structural properties. In a mechanical context, the CS/PVA/GA hydrogels exhibited a slightly higher elastic modulus than the CS/PVA/GEN hydrogels; however, GEN is five to ten thousand times less cytotoxic than GA. These results demonstrate that the physicochemical properties and structural and mechanical responses of these hybrid hydrogels can easily be tuned as a function of chemical composition; particularly, by modifying the CS/PVA proportion or varying the type/quantity of the chemical crosslinking reagent. In this context, GEN has proven to be a good alternative for improving the mechanical properties of the CS/PVA blend, thereby positioning CS/PVA/GEN as a promising hybrid hydrogel that can potentially be used in the medical (e.g., drug delivery systems and scaffolds in tissue engineering), agriculture (e.g., water controlled release systems), food and environmental industries, among others. It is important to note that hydrogels with high swelling capacity are mostly used in hygiene and agriculture fields where retention of water and aqueous solutions is expected; meanwhile for medical applications, hydrogels with low swelling capacity are generally used. Nevertheless, for each application, the hydrogels are usually custom-designed and manufactured focusing on a particular need.

Acknowledgments

This work was developed with the financial support from the PAPIIT DGAPA-UNAM program through grant IT100215. The authors are grateful to MSc. Adriana Tejeda for the X-ray measurements (IIM- UNAM), MSc. Damaris Cabrera for the TGA and DSC analyses (IIM-UNAM) and MSc. Miguel A. Canseco for the FT-IR measurements.

References

ASTM-International. (2013). *ASTM D1708-13: Standard test method for tensile properties of plastics by use of microtensile specimens*.

Baker, M. I., Walsh, S. P., Schwartz, Z., & Boyan, B. D. (2011). A review of polyvinyl alcohol and its uses in cartilage and orthopedic applications. *Journal of Biomedical Materials Research Part B*, *5*, 1451–1457.

Berger, J., Reist, M., Mayer, J. M., Felt, O., Peppas, N. A., & Gurny, R. (2004). Structure and interactions in covalently and ionically crosslinked chitosan hydrogels for biomedical applications. *European Journal of Pharmaceutics and Biopharmaceutics*, *57*, 19–34.

Bispo, V. M., Mansur, A. A. P., Barbosa-Stancioli, E. F., & Mansur, H. S. (2010). Biocompatibility of nanostructured chitosan/poly(vinyl alcohol) blends chemically crosslinked with genipin for biomedical applications. *Journal of Biomedical Nanotechnology*, *6*, 166–175.

Carmona, D., Martinez, J., Londo no, M. E., Montoya, Y., & Torres, R. (2015). Novel sensor based on polyvinyl alcohol hydrogel. In *IFMBE Proceedings, Vol. 49* (pp. 39–42).

Carreira, A. S., Ferreira, P., Ribeiro, M. P., Correia, T. R., Coutinho, P., Correia, I. J., et al. (2014). New drug-eluting lenses to be applied as bandages after keratoprosthesis implantation. *International Journal of Pharmaceutics*, *477*, 218–226.

Chawla, P., Srivastava, A. R., Pandey, P., & Chawla, V. (2014). Hydrogels: A journey from diapers to gene delivery. *Mini Reviews in Medicinal Chemistry*, *14*, 154–167.

Chuang, W. Y., Young, T. H., Yao, C. H., & Chiu, W. Y. (1999). Properties of the poly(vinyl alcohol)/chitosan blend and its effect on the culture of fibroblast in vitro. *Biomaterials*, *20*, 1479–1487.

Costa-Júnior, E. S., Barbosa-Stancioli, E. F., Mansur, A. A., Vasconcelos, W. L., & Mansur, H. S. (2009). Preparation and characterization of chitosan/poly(vinyl alcohol) chemically crosslinked blends for biomedical applications. *Carbohydrate Polymers*, *76*, 472–481.

D'Errico, G., De Lellis, M., Mangiapia, G., Tedeschi, A., Ortona, O., Fusco, S., et al. (2008). Structural and mechanical properties of UV-photo-cross-linked poly(N-vinyl-2-pyrrolidone) hydrogels. *Biomacromolecules*, *9*, 231–240.

El-Hefian, E. A., Nasef, M. M., & Yahaya, A. H. (2010). The preparation and characterization of chitosan/poly(vinyl alcohol) blended films. *E-Journal of Chemistry*, *7*, 1212–1219.

Flory, P. J. (1953). Rubber elasticity, statistical thermodynamics of polymer solutions. In P. J. Flory (Ed.), *Principles of polymer chemistry* (1st ed., pp. 432–540). Ithaca, NY, USA: Cornell University Press.

Garnica-Palafox, I., Sánchez-Arévalo, F., Velasquillo, C., García-Carvajal, Z., García-López, J., Ortega-Sánchez, C., et al. (2014). Mechanical and structural

response of a hybrid hydrogel based on chitosan and poly(vinyl alcohol) cross-linked with epichlorohydrin for potential use in tissue engineering. *Journal of Biomaterials Science. Polymer Edition*, *25*, 32–50.
Giovino, C., Ayensu, I., Tetteh, J., & Boateng, J. S. (2013). An integrated buccal delivery system combining chitosan films impregnated with peptide loaded PEG-b-PLA nanoparticles. *Colloids and Surfaces B: Biointerfaces*, *112*, 9–15.
Gupta, N. V., & Shivakumar, H. G. (2012). Investigation of swelling behavior and mechanical properties of a pH-sensitive superporous hydrogel composite. *Iranian Journal of Pharmaceutical Research*, *11*, 481–493.
He, Z., & Xiong, L. (2012). Evaluation of physical and biological properties of polyvinyl alcohol/chitosan blend films. *Journal of Macromolecular Science, Part B: Physics*, *51*, 1705–1714.
Hu, H., Xin, J. H., Hu, H., Chan, A., & He, L. (2013). Glutaraldehyde-chitosan and poly(vinyl alcohol) blends, and fluorescence of their nano-silica composite films. *Carbohydrate Polymers*, *91*, 305–313.
Hui, B., Zhang, Y., & Ye, L. (2015). Structure of PVA/gelatin hydrogel beads and adsorption mechanism for advanced Pb(II) removal. *Journal of Industrial and Engineering Chemistry*, *21*, 868–876.
Hyon, S., Chu, H., & Kitamaru, R. (1975). Structure and physico-chemical properties of polyvinyl alcohol, stretched at the amorphous state and annealed. *Bulletin of the Institute for Chemical Research*, *53*, 367–380.
Khurma, J. R., Rohindra, D. R., & Nand, A. V. (2006). Synthesis and properties of hydrogels based on chitosan and poly(vinyl alcohol) crosslinked by genipin. *Journal of Macromolecular Science – Pure and Applied Chemistry*, *43*, 749–758.
Li, C., She, M., She, X., Dai, J., & Kong, L. (2014). Functionalization of polyvinyl alcohol hydrogels with graphene oxide for potential dye removal. *Journal of Applied Polymer Science*, 131.
Liu, Y., & Kim, H.-I. (2012). Characterization and antibacterial properties of genipin-crosslinked chitosan/poly(ethylene glycol)/ZnO/Ag nanocomposites. *Carbohydrate Polymers*, *89*, 111–116.
Mansur, H. S., Costa-Junior, E., Mansur, A. A. P., & Barbosa-Stancioli, E. F. (2009). Cytocompatibility evaluation in cell-culture systems of chemically crosslinked chitosan/PVA hydrogels. *Materials Science and Engineering C*, *29*, 1574–1583.
Mathews, D. T., Birney, Y. A., Cahill, P. A., & McGuinness, G. B. (2008). Mechanical and morphological characteristics of poly(vinyl alcohol)/chitosan hydrogels. *Journal of Applied Polymer Science*, *109*, 1129–1137.
Mekhail, M., Jahan, K., & Tabrizian, M. (2014). Genipin-crosslinked chitosan/poly-L-lysine gels promote fibroblast adhesion and proliferation. *Carbohydrate Polymers*, *108*, 91–98.
Mogilevskaya, E., Akopova, T., Zelenetskii, A., & Ozerin, A. (2006). The crystal structure of chitin and chitosan. *Polymer Science Series A*, *48*, 116–123.
Muzzarelli, R. A. (2009). Genipin-crosslinked chitosan hydrogels as biomedical and pharmaceutical aids. *Carbohydrate Polymers*, *77*, 1–9.
Nath, S. D., Abueva, C., Kim, B., & Lee, B. T. (2015). Chitosan/hyaluronic acid polyelectrolyte complex scaffold crosslinked with genipin for immobilization and controlled release of BMP-2. *Carbohydrate Polymers*, *115*, 160–169.
Naveen Kumar, H. M. P., Prabhakar, M. N., Venkata Prasad, C., Madhusudhan Rao, K., Ashok Kumar Reddy, T. V., Chowdoji Rao, K., et al. (2010). Compatibility studies of chitosan/PVA blend in 2% aqueous acetic acid solution at 30 °C. *Carbohydrate Polymers*, *82*, 251–255.
Ogawa, K., Yui, T., & Miya, M. (1992). Dependence on the preparation procedure of the polymorphism and crystallinity of chitosan membranes. *Bioscience, Biotechnology, and Biochemistry*, *56*, 858–862.
Ogden, R. W. (1973). Large deformation isotropic elasticity – on the correlation of theory and experiment for incompressible rubberlike solids. *Rubber Chemistry and Technology*, *46*, 398–416.
Oliveira, R. N., Rouzé, R., Quilty, B., Alves, G. G., Soares, G. D. A., Thiré, R. M. S. M., et al. (2014). Mechanical properties and in vitro characterization of polyvinyl alcohol-nano-silver hydrogel wound dressings. *Interface Focus*, *4*, 20130049.
Omidian, H., & Park, K. (2010). Introduction to hydrogels. In R. M. Ottenbrite (Ed.), *Biomedical applications of hydrogels handbook* (pp. 1–16). New York: Springer Science.
Paradossi, G. (2013). Hydrogels formed by cross-linked poly(vinyl alcohol). In S. Dumitriu, & V. Popa (Eds.), (vol. 1) *Polymeric biomaterials: Structure and functions* (1st ed., vol. 1, pp. 37–56). Boca Ratón, FL: CRC Press.
Peppas, N. A., & Mikos, A. G. (1987). *Hydrogels in medicine and pharmacy*. (vols. 1–2) Boca Ratón, FL: CRC Press.
Sionkowska, A. (2013). Natural polymers as components of blends for biomedical applications. In S. Dumitriu, & V. Popa (Eds.), (vol. 1) *Polymeric biomaterials: Structure and function* (1st ed., vol. 1, pp. 309–340). Boca Raton, FL: CRC Press.
Tou, Z. Q., Koh, T. W., & Chan, C. C. (2014). Poly(vinyl alcohol) hydrogel based fiber interferometer sensor for heavy metal cations. *Sensors and Actuators B: Chemical*, *202*, 185–193.
Treloar, L. (2005). *The physics of rubber elasticity*. New York: Oxford University Press.
Yao, C. K., Liao, J. D., Chung, C. W., Sung, W. I., & Chang, N. J. (2012). Porous chitosan scaffold cross-linked by chemical and natural procedure applied to investigate cell regeneration. *Applied Surface Science*, *262*, 218–221.
Yin, R., Wang, K., Du, S., Chen, L., Nie, J., & Zhang, W. (2014). Design of genipin-crosslinked microgels from concanavalin A and glucosyloxyethyl acrylated chitosan for glucose-responsive insulin delivery. *Carbohydrate Polymers*, *103*, 369–376.
Yuan, Y., & Lee, R. (2013). Contact angle and wetting properties. In G. Bracco, & B. Holst (Eds.), *Surface science techniques*. Berlin: Springer-Verlag.
Zheng, H., Du, Y. M., Yu, J. H., & Xiao, L. (2000). The properties and preparation of crosslinked chitosan films. *Chemical Journal of Chinese Universities*, *21*, 812.